

Genesis of Early Cambrian phosphorite of Krol Belt, Lesser Himalaya

A. Mazumdar^{1,*} and D. M. Banerjee²

¹CSIR-National Institute of Oceanography, Dona Paula, Goa 403 004, India

²D.M. Banerjee Professor of Geology (INSA Honorary Scientist), 25, Uttaranchal Apartments, 5, I.P. Extension, Patpargunj, Delhi 110 092, India

Early Cambrian phosphogenesis in the lesser Himalaya is represented by a well-developed sequence of phosphorite, black shale and black chert with interbedded phosphatic dolomite in the Krol Belt. Prevalence of shallow marine depositional structures support shallow subtidal to intertidal depositional environment. Similar shallow marine character for Late Vendian and Early Cambrian phosphorites have been recorded from Yangtze Basin (South China), Khubshugul Basin (Mongolia), Karatau Basin (Kazakhstan), Soltaniah Basin (Iran), Tal Basin (Lesser Himalaya, India), Hazara Basin (Pakistan) and Georgia Basin (Australia). We have characterized the Tal Phosphorites of Krol Belt, Lesser Himalaya in terms of mineralogy and petrography. The phosphogenic model for the modern Peru–Chile shelf–slope phosphorite is inadequate to explain the genesis of Cambrian phosphorite. Physicochemical characters of the Cambrian phosphorites demand a shallow marine phosphorous source. Based on the available early Cambrian oceanographic models, we envisage a repeated influx of P and ¹²C rich water on to the shallow platform. Amorphous calcium phosphate (ACP) precipitated from the shallow water column overlying the sediment water interface and subsequently modified to microspherulite (micritic phosphorite). Influx of P resulted in proliferation of algal mat and stromatolites, which are found in abundance in Tal phosphorites. The algal and mudstone phosphorites were the parent material for granular phosphorites.

Keywords: Cambrian, Krol Belt, phosphorite, proterozoic, Tal Formation.

Introduction

PHOSPHORITES are chemogenic sediments which contain high amounts of phosphate-bearing minerals such as Ca-fluorapatite and/or Ca-hydroxyapatite relative to the average sedimentary rocks. Typical marine sedimentary phosphorites contain cryptocrystalline phosphate mineral called carbonate fluoroapatite represented by the generalized structural formula: $\text{Ca}_{10-a-b}\text{Na}_a\text{Mg}_b(\text{PO}_4)_{6-x}(\text{CO}_3)_{x-y-z}(\text{CO}_3 \cdot \text{F})_y(\text{SO}_4)_z\text{F}_2$. Biogeochemical significance, as well as the episodic nature of phosphorite deposits have been

widely studied. The period between late Neoproterozoic and middle Cambrian witnessed repeated phosphogenic events^{1–3}. Late Neoproterozoic phosphogenesis was followed by a major peak of extensive phosphorite deposition in the early Cambrian (Tommotian). This episode continued with decreasing evidences of phosphate formation in the middle Cambrian before tapering to an end by the upper Cambrian³. Major phosphorite deposits belonging to this time-window have been recorded from the sedimentary basins in the Yangtze (South China), Khubshugul (Mongolia), Karatau (Kazakhstan), Soltaniah (Iran), Krol Belt (Lesser Himalaya, India), Hazara (Pakistan) and Georgiana (Australia). In addition, several minor deposits of lesser economic importance have been reported from many other locations in North America, western Africa and Europe. Owing to lack of unequivocal faunal records and radiogenic dates, precise temporal correlation of these phosphorite deposits is yet to be achieved. Phosphorite rocks of these deposits share several common physicochemical characters which have a bearing on their genesis. Strikingly similar facies association (dolomite–chert–shale–phosphorite) and prevalence of shallow marine depositional characteristics, demand a broadly uniform genetic model. The depositional setting inferred for the Proterozoic and Cambrian phosphorites is apparently quite different from that of modern phosphorite forming zones such as those of Peru, Chile and Namibia offshore^{4,5}. This is primarily because most Precambrian and Cambrian phosphorites bear unequivocal imprints of shallow water deposition (peritidal) and are characterized by the preponderance of mudstone and boundstone type phosphorite⁶. Phosphogenic events through late Neoproterozoic and middle Cambrian had been linked to the contemporary oceanographic and isotopic events^{7–10}. In this article, we make a critical assessment of some of the genetic aspects of the early Cambrian (Tommotian) phosphorites of Krol Belt, Lesser Himalaya.

Geological setup

The Baliana, Krol and Tal Group sedimentary rocks represent the Neoproterozoic-early Cambrian sequence of the Krol Belt in the Lesser Himalaya¹¹. This thick pile of sedimentary cover, crops out in several discrete synclines

*For correspondence. (e-mail: maninda@nio.org)

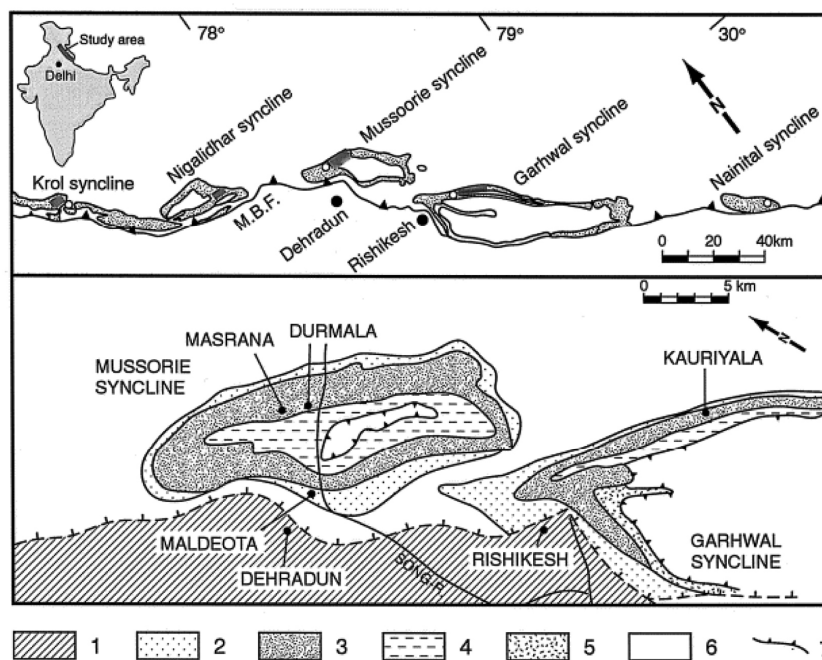


Figure 1. Geological map showing different phosphorite bearing basins of Krol Belt, Lesser Himalaya. 1, Cenozoic foreland deposits; 2, Proterozoic Blaini and Infrakrol Formations; 3, Neoproterozoic Krol Group; 4, Lower Cambrian Tal Group; 5, Subathu Formation; 6, Proterozoic pre-Blaini and other rocks in tectonic windows and 7, Thrust.

extending over a distance of 300 km (Figure 1). The basal clastic Mesoproterozoic sequence of shallow, fluvio-marine Nagthat arenites is overlain by the Neoproterozoic Blaini Group consisting of diamictite, arenite, shale and cap carbonate. The overlying Infrakrol Formation is followed by the Krol Group which is divided into Krol A, B, C, D and E Formations. Krol-A is made up of marlstone and sandstone, Krol-B of red/green shales and minor carbonates, Krol-C of limestone/dolomite with algal laminations, Krol-D of fenestral, stromatolitic dolomite with chert layers and Krol-E of argillaceous dolomite, laminated dolomite and grey/black shales. These rocks broadly reflect a supratidal to shallow-subtidal depositional milieu. Krol Group is conformably overlain by a sequence of organic rich black shale, chert and phosphorite belonging to Lower Tal Formation of the Tommotian stage. Early Cambrian succession here is characterized by assemblages of small shelly fossils such as *Anabarites* sp., *Protohertzina* sp. and *Maldeotaia* sp.¹². Nemakit–Daldynian to early Tommotian age for the Lower Tal Formation has been suggested on the basis of organic walled microfossils (acanthomorphs) and sponge spicules^{13,14}. The chert–phosphorite member is exposed in the Nigalidhar, Korgai, Mussoorie and Garhwal synclines of the Krol Belt. Maldeota, Durmala, Masrana and Bhusti–Jalikhil are among the best developed phosphorite deposits in the Krol Belt.

Analytical procedure

Petrographic studies were carried out using a polarized light microscope (Leitz). Mineralogical studies were

carried out using a Philips-PW 1130 X-ray diffractometer. Quartz was used as an internal standard for drift correction. $\text{CuK}\alpha_1$ ($\lambda = 1.5405 \text{ \AA}$) radiation was used for X-ray diffraction analysis. The instrument was operated at 50 mA and 40 kV. Structural CO_2 content of francolite was determined following peak pair method of Gulbrandsen¹⁵. The reflection pairs 410 and 004 were used for the CO_2 quantification. The equation used to calculate the structural CO_2 content is as follows

$$\text{CO}_2 \text{ (wt\%)} = 23.6341 - 14.7361 \times (\Delta^2\theta)_{004-410} \quad (1)$$

Scanning electron microscopy was carried out using SEM (Model: JEOL JSM840) at the Delhi University. Chemical composition at specific points in apatite grains of polished phosphorite samples were determined by electron probe micro analyses (EPMA: JEOL JXA-8600M Superprobe) technique at USIC, University of Roorkee. The instrument was operated at 20 nA probe current and 15 kV acceleration voltage. Electron beam diameter was adjusted to 2 μ . Apatite (Ca, P), almandine garnet (Si, Mg), kaersutite (Na) and CaF_2 (F) were used as standards.

Results and discussion

Bulk mineralogy

Carbonate fluorapatite (CFA) or francolite is the main phosphate mineral in the Tal phosphorite. Dolomite/calcite and chert are the main matrix minerals. They also occur as diagenetic veinlets. Pyrite occurs as veins, laminations

Table 1. Electron probe micro analyses and XRD based mineral chemistry data of phosphorite grains

Sample location	CaO (%)	MgO (%)	P ₂ O ₅ (%)	Na ₂ O (%)	F (%)	CO ₂ (%)
Durmala granule (DQ17) point-1	58.6	0.05	43.4	0.02	1.05	2.1
Durmala granule (DQ17) point-2	52.0	0.03	39.8	0.006	0.79	2.1
Masranagranule (M-54) point-1	55.3	0.06	41.2	0.21	0.2	2.7
Masranagranule (M-54) point-2	55.2	0.06	41.2	0.21	0.22	2.7
Apatite rim around granule (M-54)	56.2	0.035	42.3	0.14	1.0	2.7
Maldeota platy (SK-7) point-1	55.6	0.03	42.3	0.46	0.57	1.1
Maldeota platy (SK-7) point-2	57.4	0.076	40.9	0.02	0.35	1.1
Maldeota platy (SK-7) point-3	58.03	0.128	42.4	0.16	1.18	1.1

and disseminated grains. Illite, chlorite and detrital quartz grains are present in variable amounts and form an important constituent of the acid insoluble residue. The organic matter content⁹ varies from <1% to 4%. The crystal chemistry of phosphate granules is provided in Table 1.

Nature of Tal phosphorite and depositional setup

Mudstone phosphorite: Thick to thin-bedded cryptocrystalline mudstone phosphorite is a common phosphorite type in the lower Tal Formation. It is mostly structureless, although at times microscopic laminations are prominently seen. The laminations sometimes exhibit affinity to algal laminites. Presence of microphosphorite intraclasts within dolomite/limestone layers (Figure 2a) is a common feature in mudstone phosphorites. The intraclast bearing layers range from few millimetres to 10s of centimetres in thickness and show variations in the shape of the clasts. The intraclasts float in a recrystallized dolomitic matrix and the platy fragments show orientations parallel or oblique to the primary bedding planes (Figure 2b). Ripped-off phosphorite clasts just above the thick microphosphorite layer shown in Figure 2b suggest relatively high energy condition in the depositional environment. Similar structures are known from the Early Cambrian phosphorites of China, Mongolia, Russian platform and Kazakhstan. Phosphatization of the carbonate sediments is not evident in our microscopic studies. This observation is further supported by the ubiquitous presence of unaltered detrital carbonate granules and laminae within the phosphatic layers. Primary depositional features such as flat pebble or mudchip conglomerates, flaser beds, small-scale low angle cross bedding, small scale ripple marks in grainstone phosphorites, crinkled microbial laminites and stromatolites within the microphosphorite facies¹⁶ are suggestive of intertidal to shallow subtidal depositional setting for the Tal microphosphorite beds.

Granular phosphorite: Texturally, two types of granular phosphorites have been recognized in the Lower Tal Formation. The angular to partially rounded phosphate grains in carbonate matrix can be termed as wackestone.

The wackestone layers have intervening microphosphorite layers. Some phosphate grains show partial to complete replacement by carbonates and thereby possess prominent embayed margins (Figure 2c). Some grains have retained relict textures¹⁶. Complete to partial replacement of carbonate matrix and phosphate grains by secondary silica is often observed in the chert beds (Figure 2d). The grain-supported packstone type texture (Figure 2e) is suggestive of repeated reworking and winnowing before burial and lithification. The 0.05 to 0.3 mm size phosphate granules show recrystallized apatite rims around the grains. These grains sometimes show plastic deformation, featuring fractured and broken apatite rims formed during diagenetic compaction¹⁶. The aphanitic apatite rims enveloping phosphate grains (as evident from EPMA data) (Table 1) are composed of a series of light and dark coloured layers, possibly reflecting episodes of apatite precipitation (Figure 2f).

Algal mat and stromatolitic phosphorite: Phosphatic algal mats and domal stromatolites have been recorded within the phosphorite beds in both Durmala and Maldeota areas. The polished hand specimen in Figure 2g, displays evidence of repeated shallowing upward cycles characterized by microbial laminites, domal stromatolites and reworked phosphate clasts of centimeter size, which point to the shallow marine depositional environment. Microbial laminites apparently provided spaces for the trapping of phosphate granules, which are fairly small and frequently show coatings of microbial layers. Crenulated microbial laminations are suggestive of subaerial exposure (Figure 2h, i). Pyrite is associated with the algal mats as early/late diagenetic precipitates and partially replaces carbonate and phosphate clasts.

Phosphogenesis

Modern marine phosphorites are commonly observed as chemogenic cement phase (micronodules and hardgrounds) within organic rich mud^{17,18}. The process involves decomposition of organic matter¹⁸ and reduction of Fe-oxyhydroxide in the suboxic–anoxic sediments, which tend to release P into the pore waters¹⁹. This process

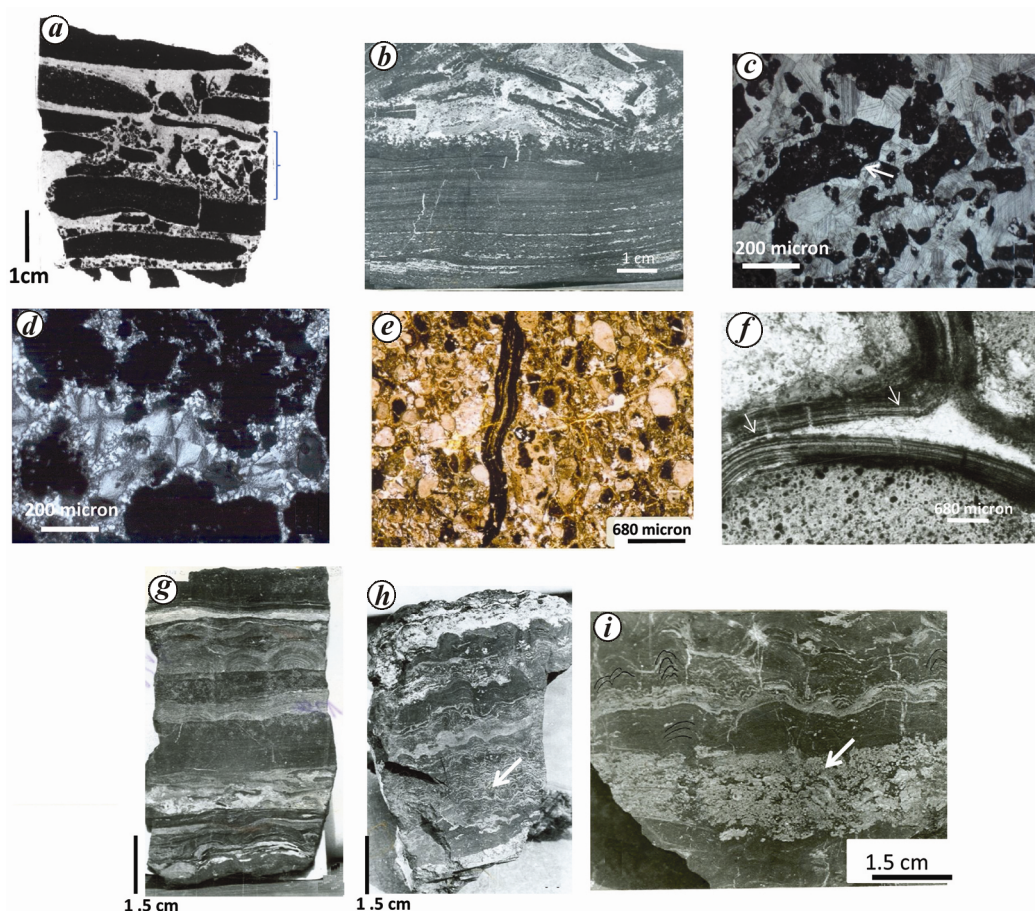


Figure 2. *a*, Layering of mudstone phosphorite and dolomite containing phosphate breccia. *b*, Flat fragments of ripped off mudstone phosphorite in dolomite matrix overlying massive mudstone phosphorite. *c*, Carbonate mud-supported irregular phosphorite grains showing embayed structure (white arrow). *d*, Corroded phosphate grains in chert matrix. *e*, Grain-supported phosphorite texture. *f*, Growth layers in apatite rim on rounded phosphate grains. Intragranular space is filled with recrystallized apatite cement. *g*, Algal mat with phosphorite. White arrow shows pyrite laminae. *h* and *i*, Alternating layers of microbial laminae, short domal stromatolites and phosphate intraclasts in carbonate matrix.

raises the dissolved inorganic phosphorous (DIP) concentrations leading to the precipitation of amorphous phosphate due to supersaturation. Subsequent diagenetic processes promote the growth of authigenic francolite²⁰ via incorporation of F^{-1} and CO_3 ions in the francolite lattice. Formation of economically mineable phosphorite beds is believed to be the result of mechanical concentration following sedimentation⁴ at times of lower sea level stands. Repeated reworking and winnowing results in the enrichment of phosphate pellets and increases the phosphorous concentrations²¹. In contrast to the modern shelf-slope phosphorites, the early Cambrian economically significant phosphorite beds bear clear imprints of rather shallow water depth, in a protected lagoonal and tidal flat condition. Based on our study and existing reports from other parts of the world, the mudstone phosphorites may be considered as the primary inorganic precipitates²². Along with the microbial mat-bound phosphates, they represent the parent material for granular phosphorites. Alternation of mudstone phosphorite and the carbonate beds and laminae at meso as well as microscopic scales, suggests fluctuations in dissolved phosphate concentration or the

degree of saturation in the shallow water column. Repeated flux of dissolved phosphate into the shallow marine milieu appears to have resulted in supersaturation, leading to the precipitation of a sparingly soluble phosphate salt, the amorphous calcium phosphate (ACP). Presence of such an amorphous phase has been demonstrated²³ through a transmission electron microscope (TEM) study of the Jurassic stromatolites. The amorphous to crystalline transformation is believed to be rapid¹⁷ and once the nuclei exceed a critical size, they grow further at a faster rate. At the early diagenetic stage, the most important activity is known to be substitution of Ca, PO_4^{3-} and/or OH^{-} ions. Substitutions of OH^{-} by F^{-} and/or Cl^{-} , PO_4^{3-} by SO_4^{2-} and/or CO_3^{2-} and Ca^{2+} by Sr^{2+} , Mg^{2+} and Na^{+} ions have been reported²⁴. All these depositional factors suggest that the ubiquitous carbonate fluorapatite is a product of the early diagenesis of amorphous calcium phosphate mud. Gulbrandsen *et al.*²⁵ experimentally demonstrated the feasibility of crystallization of carbonate fluorapatite through intermediate amorphous state in the presence of Mg^{2+} ion, which is commonly considered an inhibitor of francolite crystallization²⁶.

Influx of phosphate into the depositional basin is expected to promote rapid blooming and proliferation of the cyanobacterial mat. Natural microbial populations usually secrete large amounts of extracellular expolymers (EPS), ranging from tightly structured capsules and sheaths around cells to a more loosely bound slime that forms the matrix of microbial biofilms and mats²⁷. This characteristic of microbial mats may enable them to bind the francolite microcrysts on their surfaces, giving rise to microbial laminations. The capacity of microbiota, viz. bacteria, fungi and cyanobacterial mat-forming microphytes to trap and bind phosphate has been amply demonstrated by Soudry²⁸. Other than precipitating apatite and trapping reworked phosphate grain, the mat structures serve the purpose of stabilizing the mudstone phosphate layers against current and wave actions which may cause brecciation. Contraction of the organic layer, with a drop in phosphate concentration, makes the partially lithified mudstone phosphate vulnerable to wave and current action. Lowering of phosphate concentration in the water, promotes carbonate precipitation since phosphate is a well-known inhibitor of carbonate precipitation. This explains the observation that carbonate interlayers always contain intra-clasts of underlying mudstone phosphates.

Common association of pyrite (Figure 2 *h* and *i*) with mudstone and microbial phosphorite suggests existence of sulphate-reducing condition. Existence of thin laminae of pyrite along with algal mat suggests possible syngenetic growth of pyrite within phosphate layers, whereas veinlets of pyrite cutting across phosphate and carbonate layers and partial to complete replacement of phosphate grains by pyrite, suggest late diagenetic pyritization.

Phosphate source and Early Cambrian oceanography

A fundamental problem associated with the genetic modelling of phosphate source for late Proterozoic and early Cambrian phosphorites is their shallow marine depositional environment. Genesis for Quaternary shelf-slope phosphorites is related to coastal upwelling^{29,30} processes which greatly enhances bioproductivity in the water column. This process subsequently leads to precipitation of francolite during early diagenesis in the sediments underlying the oxygen minimum zone (OMZ). The phosphate crusts/nodules/phosphatized limestones, are apparently formed at water depths ranging from 100 to 1000 m. However, such type of phosphogenic setting cannot explain genesis of early Cambrian phosphorites with intertidal/supratidal depositional structures. This type of phosphorites were likely to have deposited in shallow epicontinental seas²². Rare earth element (REE) geochemistry of Tal phosphorite¹⁰ (and other early Cambrian phosphorites³¹) bears distinct marine signature in the form of well-defined negative Ce anomaly and seawater

like REE distribution pattern. These data suggest a marine depositional milieu^{31,32}. Underlying Krol carbonates also show seawater-like REE distribution³³. The REE pattern logically discards fluvial or continental derived phosphate mud. Widespread early Cambrian phosphogenesis reflects major changes in the chemistry and configuration of the contemporaneous world ocean³⁴. Various paleoceanographic models postulated for the Late Proterozoic and Early Cambrian^{8,35,36} suggest significant modifications notably in the redox chemistry and structure of the ocean water column. Geologic evidence suggests marked thermohaline stratification and diminished vertical circulation during the end phase of Neoproterozoic, leading to widespread anoxic condition^{34,37}. Recent studies¹⁹ have demonstrated large-scale regeneration of P in anoxic water column and sediment. Such redox-dependent phosphorous regeneration process should therefore be capable of building a reservoir of dissolved inorganic phosphorous (DIP) as discussed by a few studies^{10,38}. Phosphorous released by desorption of ferric oxyhydroxide could be additional source for DIP in such an environment. Owing to biodegradation, the dissolved inorganic carbon (DIC) in anoxic water column is expected to become enriched in ¹²C. Assuming that the redoxline separating the anoxic-oxic water was relatively shallow, transgressive or the upwelling event would bring water supersaturated in P and enriched in ¹²C on to the shallow platform leading to phosphate formation. The sharp negative C-isotopic excursion³⁸ and appearance of phosphorite at the base of Lower Tal Formation suggest an influx of ¹²C-enriched water into the depositional basin. High organic content in the phosphorites, presence of black shales and ubiquitous occurrence of pyrite, suggest eutrophication and phytoplankton bloom.

Conclusion

Early Cambrian phosphorite facies of lower Tal Formation comprises mudstone, granular and algal types which are characterized by intertidal to shallow subtidal depositional characters. Phosphatic mud possibly deposited from seawater supersaturated relative to amorphous calcium phosphate which subsequently converted to francolite via wide range of elemental/ionic substitution. The geochemical evidences support marine phosphate source possibly via upwelling/transgression of phosphate-rich anoxic water over the shallow depositional milieu during early Cambrian.

1. Cook, P. J. and Shergold, J. H., Phosphorous, phosphorite and skeletal evolution at the Precambrian-Cambrian boundary. *Nature*, 1984, **308**, 231-236.
2. Cook, P. J. and Shergold, J. H. (eds), *Phosphate Deposits of the World. Vol. 1. Proterozoic and Cambrian Phosphorites*, Cambridge University Press, Cambridge, 1986, p. 386.

3. Cook, P. J., Phosphogenesis around the Proterozoic–Cambrian transition. *J. Geol. Soc. London*, 1992, **149**, 615–620.
4. Baturin, G. N., *Phosphorite on the Sea-floor, Origin, Distribution and Composition: Developments in Sedimentology*, Elsevier, Amsterdam, 1982, p. 340.
5. Froelich, P. N. *et al.*, Early diagenesis of organic matter in Peru continental margin sediments: phosphorite precipitation. *Mar. Geol.*, 1988, **80**, 309–343.
6. Cook, P. J. and Shergold, J. H. (eds), Proterozoic and Cambrian phosphorites—nature and origin. In *Phosphate Deposits of the World, Proterozoic and Cambrian Phosphorites*, Cambridge University Press, Cambridge, 1986, vol. 1, pp. 369–390.
7. Brasier, M. D., Phosphogenic events and skeletal preservation across the Precambrian–Cambrian boundary interval. In *Phosphorite Research and Development* (eds Notholt, A. G. and Jarvis, I.), Geological Society Special Publication, London, 1990, vol. 52, pp. 289–303.
8. Donnelly, T. H., Shergold, J. H., Southgate, P. N. and Barnes, C. J., Events leading to global phosphogenesis around the Proterozoic–Cambrian transition. In *Phosphorite Research and Development* (eds Notholt, A. J. G. and Jarvis, I.), *J. Geol. Soc. London, Spec. Publ.*, 1990, **52**, 273–287.
9. Mazumdar, A. and Banerjee, D. M., Regional variations in the carbon isotopic composition of phosphorite from the Early Cambrian Lower Tal Formation, Mussoorie Hills, India. *Chem. Geol.*, 2001, **175**, 5–15.
10. Mazumdar, A., Banerjee, D. M., Schidlowski, M. and Balram, V., Rare-earth elements and stable isotopic geochemistry of Early Cambrian, Lower Tal chert–phosphorite of Krol Belt, Lesser Himalaya, India. *Chem. Geol.*, 1999, **156**, 275–297.
11. Shanker, R., Kumar, G., Mathur, V. K. and Joshi, A., Stratigraphy of Blaini, Infrakrol, Krol and Tal succession, Krol Belt Lesser Himalaya. *Indian J. Petrol. Geol.*, 1993, **2**, 99–136.
12. Brasier, M. D. and Singh, P., Microfossils and Precambrian–Cambrian boundary stratigraphy at Maldeota, Lesser Himalaya. *Geol. Mag.*, 1987, **124**, 323–345.
13. Mazumdar, A. and Banerjee, D. M., Siliceous sponge spicules in the Early Cambrian chert–phosphorite member of the Lower Tal Formation, Krol Belt, Lesser Himalaya. *Geology*, 1998, **26**, 899–902.
14. Tiwari, M., Organic-walled microfossils from the chert–phosphorite member, Tal Formation, Precambrian–Cambrian Boundary, India. *Precamb. Res.*, 1999, **97**, 99–113.
15. Gulbrandsen, R. A., Relation of carbon dioxide content of apatite of the Phosphoria Formation to regional facies. *US Geol. Prof. Paper*, 1970, **700B**, 9–30.
16. Mazumdar, A., Petrographic and geochemical characterization of the Neoproterozoic–Cambrian succession in a part of the Krol Belt, Lesser Himalaya, University of Delhi, Ph D thesis, 1996, p. 246.
17. Krajewsky, K. P. *et al.*, Biological processes and apatite formation in sedimentary environment. In *Concepts and Controversies in Phosphogenesis* (ed. Follmi, K. B.), *Eclogae Geol. Helvetica*, 1994, **87**, 701–745.
18. Schuffert, J. D., Kastner, M. and Jahnke, A. R., Carbon and phosphorous burial associated with modern phosphorite formation. *Mar. Geol.*, 1998, **146**, 21–31.
19. Ingall, E. D. and Jahnke, R., Evidence for enhanced phosphorus regeneration from marine sediments overlain by oxygen depleted waters. *Geochim. Cosmochim. Acta*, 1994, **58**, 2571–2575.
20. Follmi, K. B., The phosphorous cycle, phosphogenesis and marine phosphate-rich deposits. *Earth Sci. Rev.*, 1996, **40**, 55–124.
21. Follmi, K. B., Condensation and phosphogenesis: example of Helvetic mid Cretaceous (northern Tethyan margin). In *Phosphorite Research and Development* (eds Notholt, A. J. G. and Jarvis, I.), *J. Geol. Soc. London, Spec. Publ.*, 1990, **52**, 237–252.
22. Sheldon, R. P., Ancient marine phosphates. *Ann. Rev. Earth Planet. Sci.*, 1981, **9**, 251–284.
23. Sanchez-Navas, A. and Martin-Algarra, A., Genesis of apatite in phosphate stromatolites. *Eur. J. Mineral.*, 2001, **13**, 361–376.
24. Nathan, Y., The mineralogy and geochemistry of phosphorites. In *Phosphate Minerals* (eds Nriagu, J. O. and Moore, P. B.), Springer, Heidelberg, 1984, pp. 275–291.
25. Gulbrandsen, R. A., Roberson, C. E. and Neil, S. T., Time and the crystallization of apatite in seawater. *Geochim. Cosmochim. Acta*, 1984, **48**, 213–218.
26. Martens, C. S. and Harris, R., Inhibition of apatite precipitation in marine environment by magnesium ions. *Geochim. Cosmochim. Acta*, 1970, **34**, 621–625.
27. Decho, A. W., Microbial expolymer secretions in ocean environments: Their role(s) in food webs and marine processes. *Oceanogr. Mar. Biol. Annu. Rev.*, 1990, **28**, 73–153.
28. Soudry, D., Microbial phosphate sediment. In *Microbial Sediments* (eds Riding, R. E. and Awramik, S. M.), Springer-Verlag, Berlin, Heidelberg, 2000, pp. 127–136.
29. Suess, E., Phosphate regeneration from sediments of the Peru continental margin by dissolution of fish debris. *Geochim. Cosmochim. Acta*, 1981, **45**, 577–588.
30. Rao, V. P. *et al.*, A comparative study of Pleistocene phosphorites from the continental slope off western India. *Sedimentology*, 2000, **47**, 945–960.
31. Ilyin, A. V., Rare-earth geochemistry of ‘old’ phosphorites and probability of syngenetic precipitation and accumulation of phosphate. *Chem. Geol.*, 1998, **144**, 243–256.
32. Jarvis, I. *et al.*, Phosphorite geochemistry: State-of-the-art and environmental concerns. *Eclogae Geol. Helvetica*, 1994, **87**, 643–700.
33. Mazumdar, A., Tanaka, K., Takahashi, T. and Kawabe, I., Characteristics of rare earth element abundances in shallow marine continental platform carbonates of Late Neoproterozoic successions from India. *Geochem. J.*, 2003, **37**, 277–289.
34. Brasier, M. D., Global ocean–atmosphere change across the Precambrian–Cambrian transition. *Geol. Mag.*, 1992, **129**, 161–168.
35. Logan, G. A., Hayes, J. M., Hlेशima, G. B. and Summons, R. E., Terminal Proterozoic reorganisation of biogeochemical cycles. *Nature*, 1995, **376**, 53–56.
36. Kimura, H., Matsumoto, R., Kakuwa, Y., Hamdi, B. and Zibaseresht, H., The Vendian–Cambrian $\delta^{13}\text{C}$ record, North Iran: evidence for overturning of the ocean before the Cambrian explosion. *Earth Planet. Sci. Lett.*, 1997, **147**, 1–7.
37. Banerjee, D. M., Schidlowski, M., Siebert, F. and Brasier, M. D., Geochemical changes across the Proterozoic–Cambrian transition in the Durmala phosphorite mine section, Mussoorie Hills, Garhwal Himalaya, India. *Paleogeogr., Paleoclimatol., Paleoecol.*, 1997, **132**, 183–194.
38. Mazumdar, A. and Banerjee, D. M., Regional variations in the carbon isotopic composition of phosphorite from the Early Cambrian Lower Tal Formation, Mussoorie Hills, India. *Chem. Geol.*, 2001, **175**, 5–15.

ACKNOWLEDGEMENTS. A.M. acknowledges Director, CSIR-NIO for permission to publish the manuscript. Research fellowship to A.M. in the form of CSIR-JRF during 1992–96 at University of Delhi is also acknowledged.